

TURBOJET ANALYTICAL MODEL DEVELOPMENT AND VALIDATION

S. Chiesa*, G. Medici*, M. Balbo**

*Politecnico di Torino, **Alenia Aermacchi

sergio.chiesa@polito.it; giovanni.medici@polito.it; massimo.balbo@alenia.it

Keywords: *Turbojet; Steady State; Transient; Thrust Vectoring; CFD*

Abstract

This paper describes the modeling and validation procedure of a single shaft turbojet engine. The model aim is to provide detailed predictions of the flow's properties at nozzle outlet. Those predictions will be used to design a thrust vectoring system for the engine, and the flight dynamics control laws of the aircraft.

The first phase of the analysis explains the design and development a more detailed engine deck. The engine to model is a single shaft turbojet. The software developed calculates the turbojet performances in steady state; boundary conditions of the turbojet may be modified according to the engine-operating envelope.

During the second phase of the analysis, the transient model was developed. Dropping the work compatibility equation, and introducing the angular acceleration and inertial moments allow to model the engine vs. time behavior.

By using the data calculated through the steady state and transient 1-D models, the CFD model could be properly designed. The model defines the flow field going from the turbine's outlet through the nozzle to the turbojet plume downstream. In this way the estimation of the forces and moments acting on the thrust vectoring vanes can be calculated. The three models were validated using test bench data, synthetic data (previous steady state engine decks) and flight test data.

[6], [11]). In particular in order to study a thrust vectoring Unmanned Aerial Vehicle (UAV) application, an initial survey on a turbojet turbine and nozzle performances was conducted. The turbojet engine studied pushes the Alenia Aermacchi's Sky-X UAV, a technological demonstrator (Fig. 1). In literature there are many examples of turbojet steady state modeling methods [7], and [10], some of them have been developed in order to calculate transients too [14]. The models presented in this paper are based on such methods; to validate them real turbojet engine data (data calculated through a computer deck software, test bench data, and flight data) was used.



Fig. 1. Sky-X UAV

This section introduces the research; in the second part of the paper the 1-D, steady state and transient model is described, while the third section contains the CFD model. The latter uses extensively the results of 1-D models in order to define the boundary conditions. In the last part results are reported and commented.

1 General Introduction

Since 2010 Alenia Aermacchi (joined with Politecnico di Torino) is offering an Industrial Ph.D scholarship program, in order to work on some of the company's research fields (i.e. [4],

2 1-D Models

In the first phase of the development a steady state analytical model was designed. The model was built to obtain a more detailed engine deck.

The engine to model is configured with: single shaft, three stage axial compressor (fixed geometry, without any Inlet Guide Vanes IGV), single stage turbine, annular combustion chamber, fixed nozzle, pure turbojet. The simple configuration of the gas turbine, allows to model several components maps (that are unknown) by using an analytical deck [10], and [13]. Since many components lack of detailed information few simplifications were introduced in the model.

2.1 Steady State Model Layout

The software developed, based on Matlab, models a steady state, variable RPM and boundary conditions turbojet. The program calculates engine performances (e.g. mass flow rate, temperature, pressure...), in every stage. It is a 1-D (one dimensional) model, meaning that the engine was cut stage by stage in the longitudinal plane (Fig. 4), and every property is calculated as a mean value in each stage.

Matlab programming language is used due to its fast implementation yet powerful routines and matrix management tools. During the calculation the isentropic coefficient, specific heat coefficient, and combustion chamber Temperature rise values depend upon Temperature and fuel/air ratio. This choice affects the algorithm process flow (introduces few iterations), but the overall CPU requirement of the algorithm is modest, and allows real-time calculation. The model can be controlled through a GUI (Fig. 2), that contains the boundary conditions parameters to set: altitude, and temperature relative to ISA standards, Mach (Ma), Fuel lower heating value (H_u), extracted power (P_e), percent of bleed air flow ($\beta_{\%}$), and air intake isentropic efficiency (η_{in}).

Once every parameter is set, a routine verifies that the analysis point requested lies inside the engine envelope (Fig. 3). The software is modular, and its boundary condition initialization procedure allows it to be very flexible and customizable. It is possible, for example, to modify the operating envelope, by introducing the new conditions in a separate text file. Other engine internal parameters, such as

efficiencies, and iteration parameters, can be adjusted in a separate input file as well.

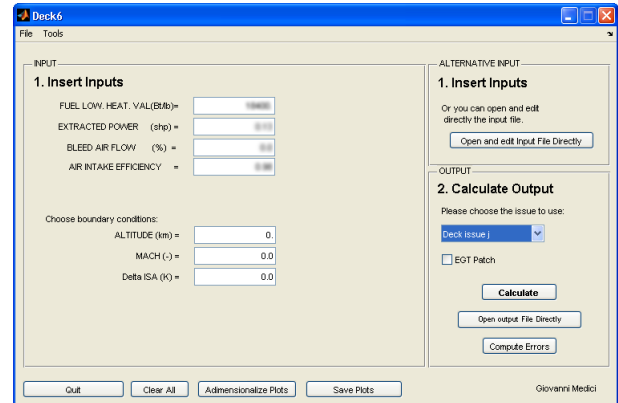


Fig. 2. Steady State Model GUI

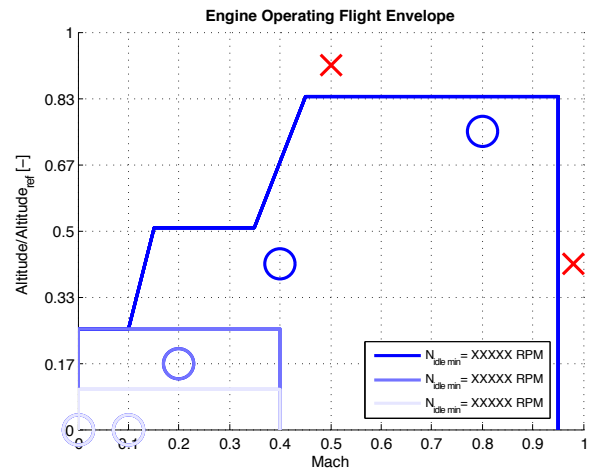


Fig. 3. Engine Operating Flight Envelope

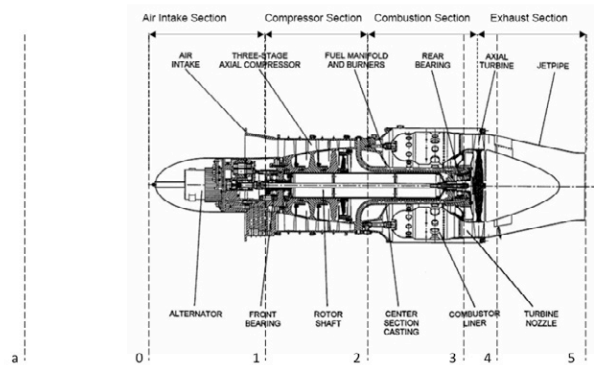


Fig. 4. Turbojet stage numbering

2.2 Steady State Model Algorithm

Off-design equilibrium running calculation is based on satisfying the flow and work compatibility between the components [12]:

- (a) The user chooses the boundary conditions (altitude, Mach, and variation from the ISA

day ΔT_{ISA}). Air intake's inlet total temperature (T_0^0) is calculated through (1), where (γ_0) is the isentropic coefficient in air intake's inlet section, (Ma) is the Mach number at air intake inlet section and (T_1^0) is the total temperature at air intake outlet section (the flow starting at infinite and going through the air intake does not exchange heat and work thus the total temperature remains constant):

$$T_0^0 = T_1^0 = T_a \cdot \left(1 + \frac{\gamma_0 - 1}{2} Ma^2\right) \quad (1)$$

There are total pressure losses, due to air intake's isentropic efficiency (η_{in}), in the stages 0-1. Total temperature and intake efficiency gives air intake's outlet total pressure (p_1^0) (2):

$$p_1^0 = p_a \cdot \left[1 + \eta_{in} \left(\frac{T_1^0}{T_a} - 1\right)\right]^{\frac{\gamma_0}{\gamma_0 - 1}} \quad (2)$$

- (b) By picking a compressor constant-speed-line on the compressor characteristic, compressor pressure ratio $\frac{p_2^0}{p_1^0}$, corrected airflow $\frac{m\sqrt{T_1^0}}{p_1^0}$, and efficiency (η_c) of the compressor can be defined.
- (c) The compressor total temperature ratio can be calculated through the (3):

$$\Delta T_{1,2}^0 = \frac{T_1^0}{\eta_c} \cdot \left[\left(\frac{p_2^0}{p_1^0}\right)^{\frac{\gamma-1}{\gamma}} - 1 \right] \quad (3)$$

- (d) Nozzle map can be simplified as a single line characteristic map, and since the turbine characteristic does not change considerably with the RPM, a single line characteristic map can be used for the turbine too.
- (e) Afore mentioned simplification allows an easier calculation of the complete turbojet cycle. In particular for a given compressor

pressure ratio, the pressure ratio of the gas-generator turbine can be found. This approximation effectively fixes the values

of corrected turbine mass flow, $\frac{m\sqrt{T_3^0}}{p_3^0}$, and turbine temperature ratio, $\frac{\Delta T_{3,4}^0}{T_3^0}$.

- (f) In this way a single iteration is sufficient to find the equilibrium running point on each compressor constant speed line.
- (g) The compressor and turbine sides are linked by equations (4) and (5):

$$\frac{\Delta T_{3,4}^0}{T_3^0} = \frac{\Delta T_{1,2}^0}{T_1^0} \cdot \frac{T_1^0}{T_3^0} \cdot \frac{c_{p,12}}{\eta_{mech} c_{p,34}} \quad (4)$$

$$\frac{m\sqrt{T_3^0}}{p_3^0} = \frac{m\sqrt{T_1^0}}{p_1^0} \cdot \frac{p_1^0}{p_2^0} \cdot \frac{p_2^0}{p_3^0} \cdot \frac{\sqrt{T_3^0}}{\sqrt{T_1^0}} \cdot \frac{m_3}{m_1} \quad (5)$$

- (h) The iteration matches the $\frac{\Delta T_{3,4}^0}{T_3^0}$ value.

By estimating compressor and turbine's equilibrium points, every property of each turbojet's stage can be calculated. The tool iterates on each isentropic coefficient and on the constant pressure heat coefficients (c_p).

The original compressor map shows only few constant speed lines, a compressor map scale routine was developed in order to refine the compressor characteristic map. Thanks to the lookup table the plot of a property with respect to the RPM results smoother.

During the development of this tool several turbojet's unknowns had to be estimated. The general map of a component (compressor, turbine, nozzle) was usually available, or could be calculated, but the components' efficiencies had to be estimated. By choosing accordingly the components efficiencies, using reference engine examples, a close match with the experimental turbojet data is achieved.

2.3 Steady State Model Output

The steady state model allows calculating 56 parameters on five stages of the turbojet, while the original deck could only calculate 12

parameters. The source code can be accessed and adjusted as desired (in order to adapt it to a different engine). The model provides various plot tools that allows creating comparison between different simulations. For example it is possible to check the way the turbojet cycle changes due to the variation of air intake efficiency, Mach, or altitude.

Fig. 5, and Fig. 6, depict a comparison between two versions of the original deck and the actual steady state model. The figures show two of the most important turbojet engine's properties: thrust, and airflow. Table 1 summarizes the boundary conditions used in the comparison (Sea Level Standard, SLS). Results are presented with respect to the reference value of each property. The trend of the steady state model matches the one of the original decks.

The original deck used text files as input and output. This kind of format forces data management to be performed only manually (frustrating) or by a text file parsing routine (that could give rise to errors due to particular text formatting of the output file). In order to overcome this flaw the developed tool outputs Data that can be saved and accessed.

Table 1. Sea level standard and cruise boundary conditions

H_u	42800 [kJ/kg]	η_{in}	0.98 [-]
P_e	0.1 [kW]	ΔT_{ISA}	0 [K]
SLS		Cruise	
h	0 [km]	h	5 [km]
M_a	0 [-]	M_a	0.3 [-]

2.4 Transient Model

During the second phase of the analysis, the transient model was developed. The transient model calculates Engine's dynamics (properties variation vs. time), by dropping the work compatibility equation, and introducing the angular acceleration and inertial moments. The transient model uses the same Matlab function developed for the steady state to calculate stage by stage properties, while the time depending dynamics are calculated using Simulink. The model is 1-D and does not include any

information on the wall temperatures (no wall temperature inertia has been modeled).

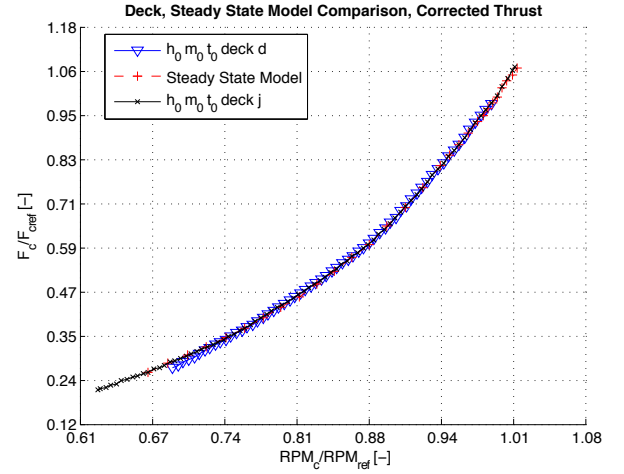


Fig. 5. Sea Level Standard Corrected Thrust.

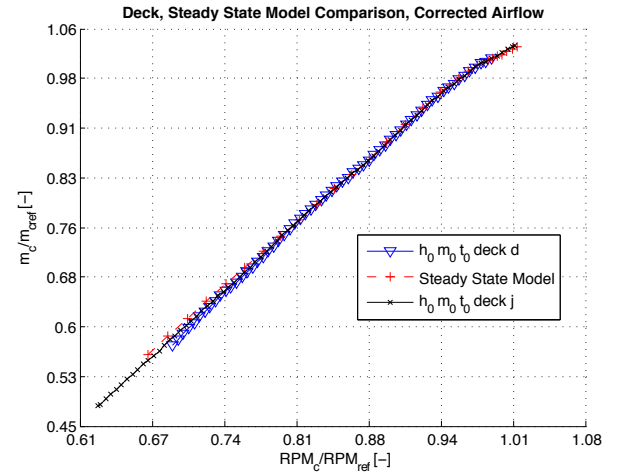


Fig. 6. Sea Level Standard Corrected airflow.

2.5 Transient Model Algorithm

In the transient model while the flow compatibility holds, work compatibility between compressor and turbine drops. The net-work between the two components induces the turbojet spool to accelerate or decelerate. The Newton's Second Law of Motion can be used to relate compressor's acceleration and the excess of torque (ΔG):

$$\Delta G = J \cdot \dot{\omega} \quad (6)$$

In equation (6) the angular acceleration of the rotor ($\dot{\omega}$) is known, the polar moment of inertia (J) was estimated using a dry crank test data. Initially the turbojet engine was accelerated to a known RPM speed. The torque

(C_{known}) was then removed and leaving the engine's spool free to rotate. By knowing the time the engine takes to stop, its polar moment of inertia was estimated (7).

$$C_{known} = J \cdot \dot{\omega} = J \cdot \frac{d\omega}{dt} \approx J \cdot \frac{RPM_{drycrank}}{t_{tostop}} \quad (7)$$

The torque excess can be written considering turbine and compressor loads (8):

$$\Delta G = G_t - G_c \quad (8)$$

Since turbine and compressor's power can be written as (9), and (10):

$$P_t = \eta_m (\dot{m}_a + \dot{m}_f) \cdot c_{p,34} \cdot \Delta T_{3,4}^0 \quad (9)$$

$$P_c = \dot{m}_a \cdot c_{p,12} \cdot \Delta T_{1,2}^0 \quad (10)$$

The torque excess can be calculated by using the (11):

$$\Delta G = \frac{\eta_{mech} (\dot{m}_a + \dot{m}_f) c_{p,34} \Delta T_{34}^0}{2\pi N} + \frac{\dot{m}_a c_{p,12} \Delta T_{12}^0}{2\pi N} \quad (11)$$

Where ($c_{p,12}$) and ($c_{p,34}$) are the constant pressure heat coefficients related to the compressor and the turbine; while airflow mass and fuel flow mass are (\dot{m}_a) and (\dot{m}_f). Now by knowing the polar moment of inertia and the simulation's time step is possible to calculate the transient running points of the turbojet. Due to the simple geometry of the engine, and relative slow dynamics (65% 100% slam takes 6 – 8 seconds), the volume inside each component can be assumed constant, so that pressure and temperature change instantly and mass conservation holds.

The basic engines dynamics are defined by the equations described before, but the real turbojet contains an Engine Control Unit (ECU), that manages fuel flow depending on thermal or mechanical constraints. By analyzing the engines time histories an elementary ECU was modeled in Simulink. The ECU block changes the fuel flow according to the RPM. When it

exceeds 98%, and the engine is accelerating, the ECU dumps the fuel flow ramp. When the Exhaust Gas Temperature (EGT), or its derivative, exceeds a threshold the ECU cuts 10% of the fuel flow.

2.6 Transient Model GUI

The layout of the model differs slightly from the steady state one, as it must provide the feature of changing the boundary conditions during the simulation (Fig. 7 and Fig. 8). The Simulink environment is particularly effective for the simulation of controllers and logics, such as Engine Control Unit [1], [5], [8], and [9].

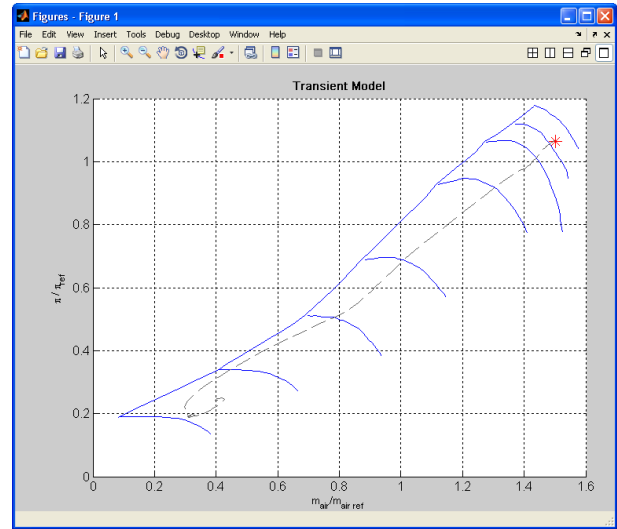


Fig. 7. Transient Model Compressor Map.

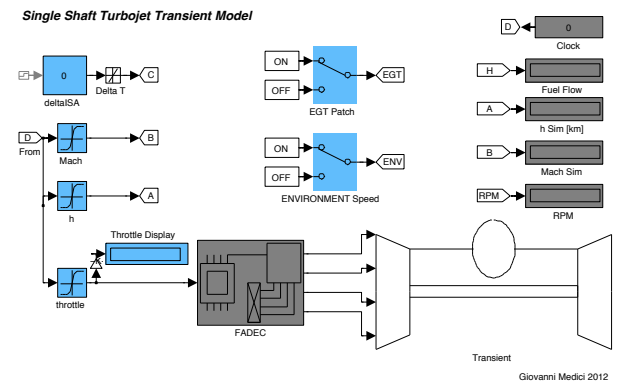


Fig. 8. Transient Model GUI

During the simulation the GUI shows a picture of the compressor's map (Fig. 7). A red star, indicating the current turbojet running point, moves in agreement to the actual engine's mechanical dynamics, leaving behind a trail (gray dashed line). The post-processing tools

allow plotting every property with respect to the simulation time; comparison between multiple data sets is also supported.

2.7 Validation of the Models

For both models great accuracy has been found during the validation phase. The 1-D steady state model shows an estimation error module lower than 4% inside the flight envelope (Fig. 5, and Fig. 6, SLS case).

Several simulations were performed by giving real flight data (i.e. Engine Throttle Command, Altitude, Speed) as input, to compare flight data to the calculated outputs. The trend lies well within the engines scattering band (3 – 4 %). The transient model’s error (time delay) is less than one second (as shown in Fig. 9). The plot depicts the time history of the engine throttle command (dashed black line), the real engine flight data (solid blue line), and the model result data (solid red line).

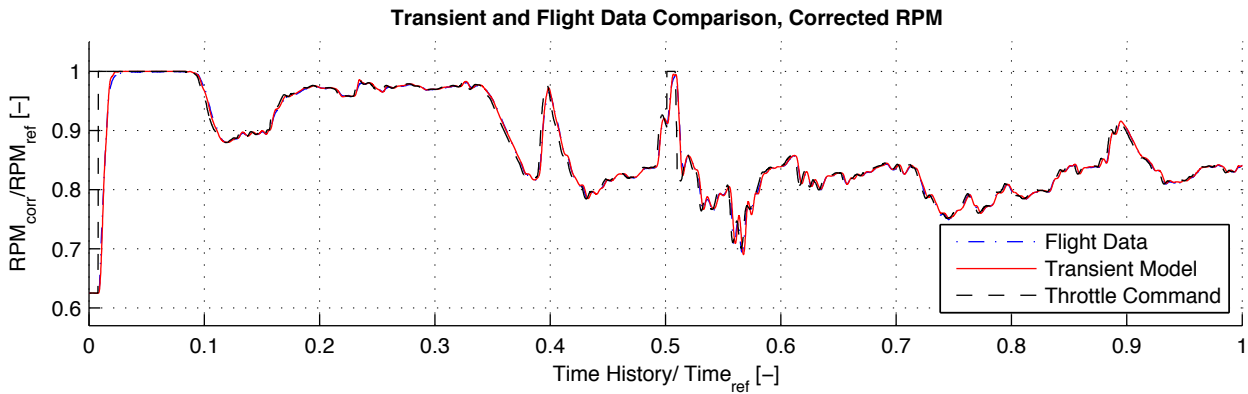


Fig. 9. Transient Model Corrected RPM Comparison.

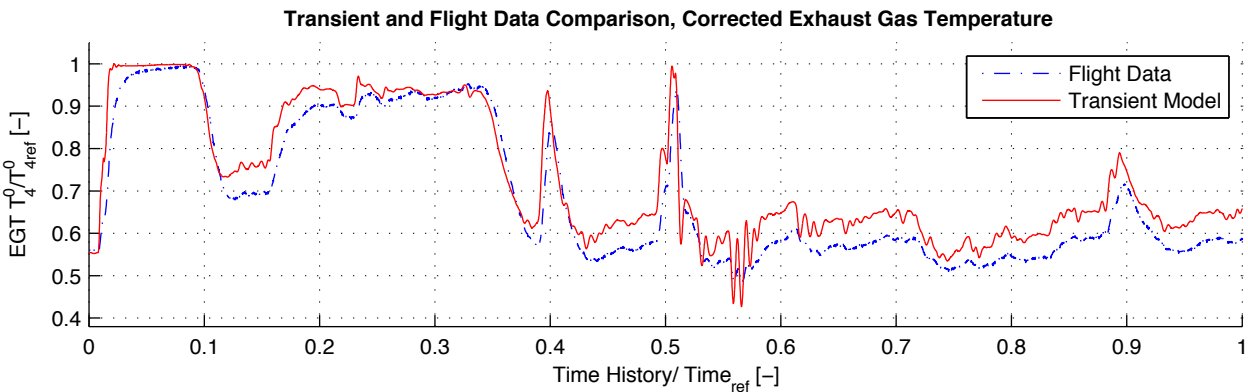


Fig. 10. Transient Model Exhaust Gas Temperature Comparison

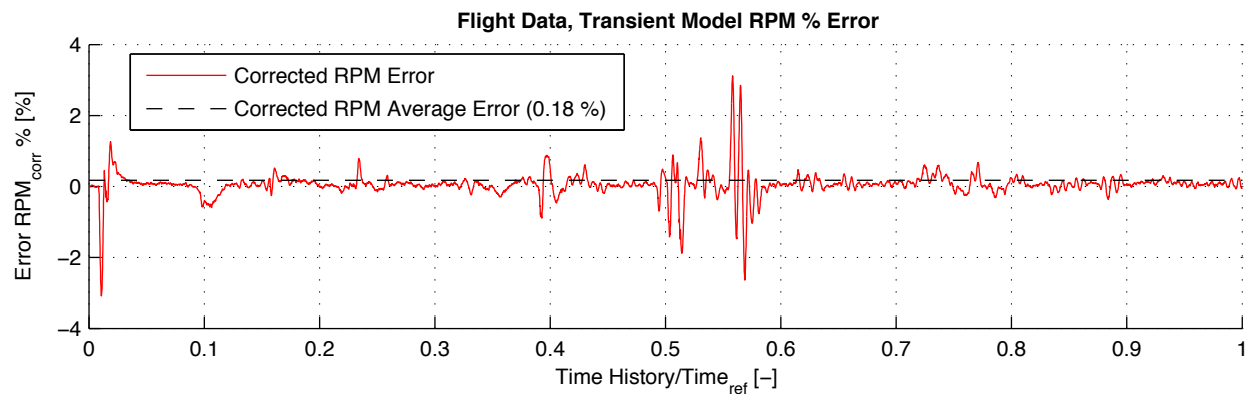


Fig. 11. Transient Model RPM error.

The two time histories are almost overlapped. There are only minor differences in the RPM time history. Exhaust gas temperature plot (Fig. 10) shows a different behavior, since the internal thermal inertia of the components is not modeled. The max error with the respect to the RPM is 4% with mean value of 0.18% (Fig. 11). In order to verify the consistency between the transient model and the steady state model, a comparison has been made. By introducing a slow accelerating RPM command in the transient model, a quasi-equilibrium simulation can be performed (Fig. 12). The models are almost identical, the minor differences between the models, may be caused from the custom ECU developed in the transient model.

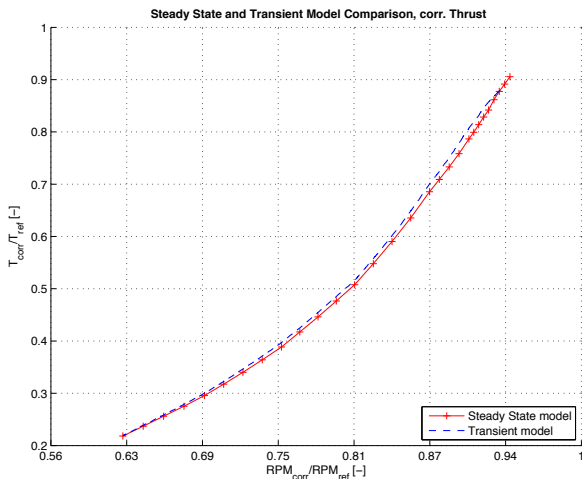


Fig. 12. Transient, steady state model comparison, corrected thrust.

3 CFD Model

The detailed knowledge of the turbine disk performances, obtained through the 1-D models enabled the set-up of a CFD model.

Its purpose is to calculate the fluid properties just outside the nozzle exit, in the free stream. The final goal of this research is to design a Thrust Vectoring System (TV), for this reason a deep understanding of the fluid dynamics in the nozzle outlet section is required. The integration of the TV system into the airplane led to some mechanical constraints, for this reason a configuration based on three vanes was used. The thrust vectoring vanes are displaced of 90° each, leaving the upper quarter

without any cover (Fig. 13). During the thrust vectoring vane design phase several wind tunnel tests were performed on scaled models. Within the framework of an internship, an undergraduate student of Politecnico di Torino and Alenia specialist, carried out this work.

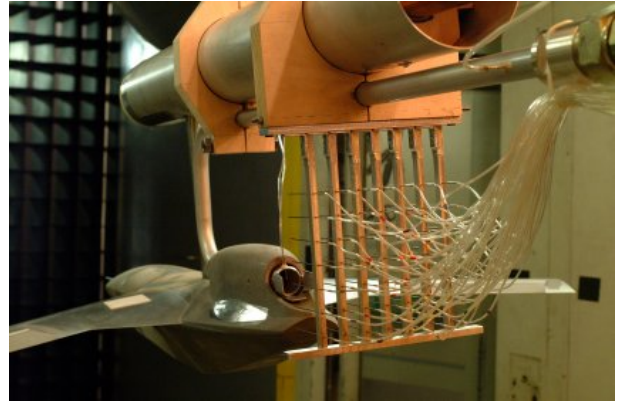


Fig. 13. Wind tunnel tests – scaled model.

3.1 CFD 2-D

In the first step of the CFD model development, a simpler 2-D axial symmetric model was created to perform a baseline performance comparison with the 1-D model.

The CFD model sets up on the turbine disk the mass flow rate and temperature conditions that have been calculated in the 1-D model. The geometry of the model contains a simplified engine nacelle, the engine nozzle and the engine diverter (Fig. 14).

The validation point is placed on the nozzle exit stage. The most important properties of the flow were compared and the resulting plots are depicted in Fig. 15 and Fig. 16. In the figures, the red (and blue) stars describe the CFD results, while the solid blue (and black) lines describe the 1-D calculated values. Thrust and Exhaust Gas Temperature (EGT) trends are in good agreement between the two analyses. In particular the EGT plot shows the mean value (solid black line / red stars) and the value detected from the EGT sensor probe (solid blue line / blue stars). The probe detects a temperature considerably higher than the average one.

By analyzing the plume close to the nozzle exit the general shape of the thrust-vectoring vane could be designed. The design was

constrained by the integration of the actuation system in the nozzle outlet zone. The main concern was to achieve a "clean" configuration, which results in lower drag losses. Several engine-running points were investigated during the 2-D CFD model analysis, in particular to identify engine chocking condition.

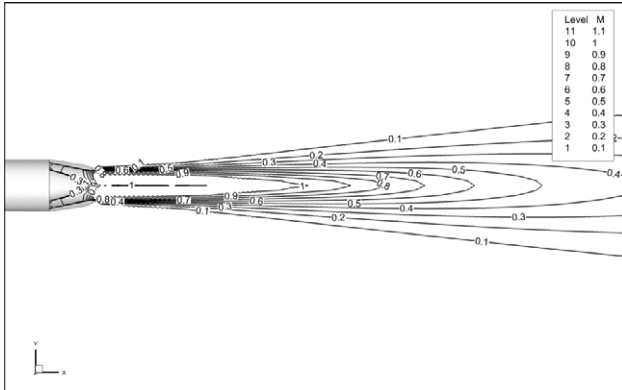


Fig. 14. CFD 2-D Mach Iso lines

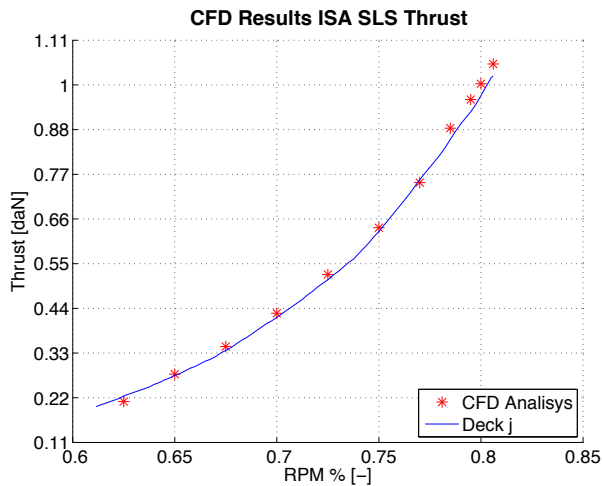


Fig. 15. Thrust comparison, 1-D and 2-D model

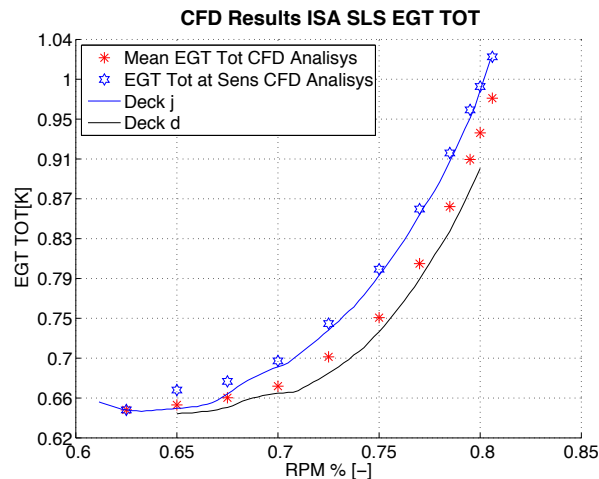


Fig. 16. EGT comparison, 1-D and 2-D model

3.2 CFD 3-D with Thrust Vectoring

The final step of the analysis led to the design of the 3-D CFD model. Once the 2-D model case check was satisfied, several 3-D configurations were analyzed (Table 2).

The model (Fig. 17) contains the engine nacelle, nozzle convergent and diverter, and the thrust vectoring system, with three vanes (Left, Bottom and Right vane). The CFD domain is quite big (cylinder: radius 50 m, and length 100 m), and the average number of element is around 3 millions. The engine nozzle was placed 10 m inside the mesh, in order to enable the airflow around the engine nacelle to develop correctly. Every mesh was solved used Navier Stokes.

Table 2 collects the several configurations that were investigated. Each mesh was solved both in SLS and Cruise condition. In the latter the sideslip effect was investigated too. The first case is used as reference case, and its results are compared with the 1-D and 2-D models. For the others the deflection of the Left, Right and Bottom vane is reported in degrees.

Table 2. Thrust Vectoring Vane Deflection.

ID	Deflection	Left	Right	Bottom
1		--	--	--
2		0	0	0
3		7.5	7.5	0
4		7.5	7.5	5
5		15	7.5	0
6		15	15	0
7		15	15	10
8		20	20	5
9		25	25	0
10		25	25	-10
11		0	0	7.5
12		0	0	15
13		0	0	25

3.3 CFD 3-D Results

The vane deflection envelope was verified and showed that a sufficient amount of thrust deflection can be obtained in SLS and cruise condition.

The aim of the proposed thrust-vectoring configuration is to maximize lateral-directional effectiveness; in the longitudinal plane pitch trim may be sufficient.

CFD results are satisfactory, and are presented in Fig. 18 and Fig. 19. In those figures, several patch are stacked (filled with gray gradient colors): SLS 100% RPM (filled dark gray, black solid line), Cruise @ RPM 100% sideslip angle, (β), $\beta = 0^\circ$ (filled light gray, black solid line), Cruise @ RPM 100%, $\beta = 20^\circ$ (filled dark gray, black dash dot line), SLS @ idle (filled dark gray, black dash dot line). Close to the plot there are the pictures (nozzle icons) of the test points; the labels describe the deflections angles of the vanes (i.e. L0R0B0 means Left Vane 0° , Right Vane 0° and Bottom Vane 0°). Deflection angle is calculated starting from the axial force and radial force of the deflected flow. The ratio between axial force of the deflected flow, and the un-deflected thrust provides the thrust vectoring effectiveness coefficient. The reference system (x,y,z) is body axis.

Thrust deflection angle is in agreement with ([1], and [2]) and shows similar trend in lateral-directional plane. Sideslip effect is negligible when compared to the average deflection component.

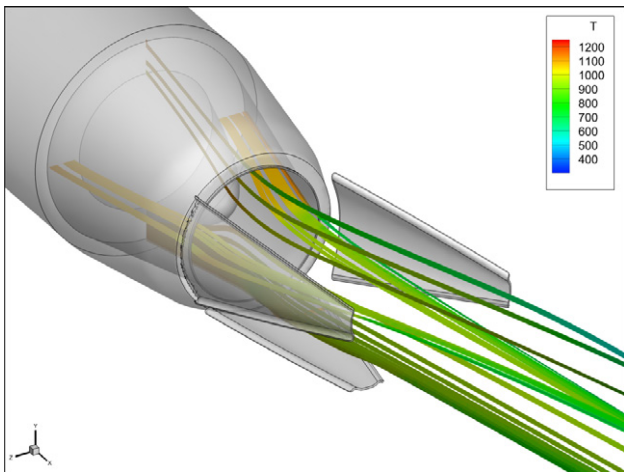


Fig. 17. CFD 3D Thrust Vectoring Streamlines Temperature colored.

Thrust vectoring system outputs lateral forces depending on the throttle settings (in particular Nozzle Pressure Ratio, NPR), regardless of the speed, this enables the system to generate a considerable lateral force even at low (including zero) airplane speed. This enhancement takes place in the takeoff and approach conditions, which are critical in the airplane envelope.

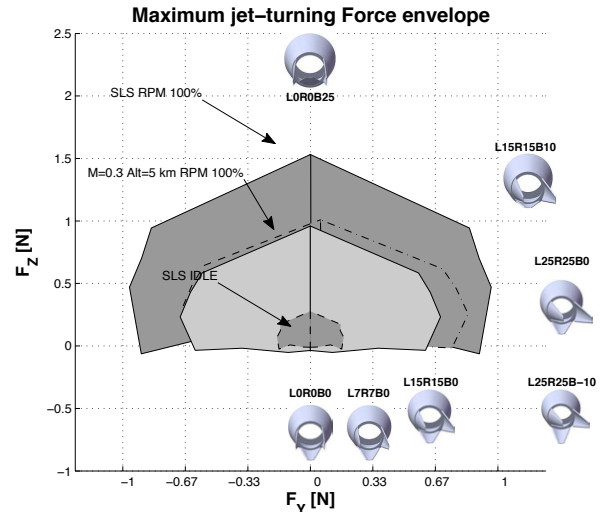


Fig. 18. CFD 3D Thrust Vectoring Forces.

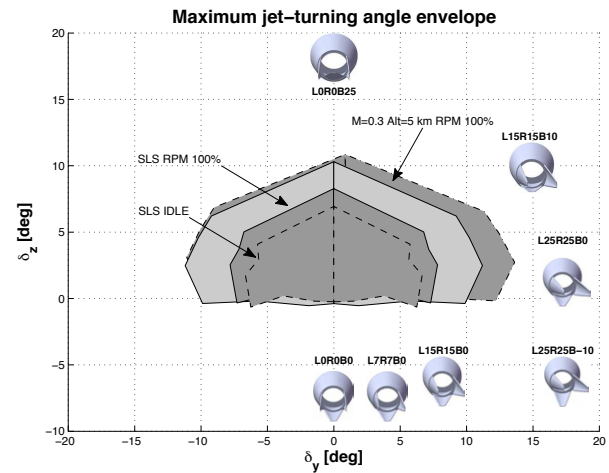


Fig. 19. CFD 3D Thrust Vectoring thrust deflections angles.

4 Conclusion

Through the development of those models, much information on the engine dynamics has been found. In particular many components' efficiencies have been estimated. A detailed analytical engine deck has been developed. The analysis started with a minimum set of known

values (very limited in terms of stages and properties), and led to a detailed 1-D steady model.

By using the same model (neglecting the compressor turbine work balance, while introducing the angular acceleration), a 1-D transient model has been developed, and validated.

The two models calculate 56 parameters, while the previous turbojet deck provided only the 12 most important ones. Engine transient performances can be calculated and critical engine operation envelope can be defined with a better degree of detail (in particular during transients). The transient model error lies inside the engine performances scattering band. The knowledge of the engine mean values stage by stage led to the definition of several CFD models.

Thanks to the CFD models plume analysis and thrust vectoring vanes design was possible. The final three vanes design produces satisfactory trim pitch, and lateral-directional thrust vector deflection. The results are in agreement with the NASA reports ([1], and [2]). In the lateral-directional plane the thrust vectoring effectiveness allows to investigate a reduced tail or even tail-less configuration, which could reduce the radar footprint of the UAV, enhance its stealth capabilities and improve its flight envelope.

Acknowledgements / Copyright Statement

The present work has been performed through a close cooperation with Alenia Aermacchi S.p.A. and through the use of Confidential Information and Data, property of Alenia Aermacchi S.p.A., which remains the sole owner of all such relevant IP rights. The result of the present work shall be, therefore, property of Alenia Aermacchi S.p.A. Authors wish to thank Dr. Renzo Bava, Dr. Marco Ferrero and Dr. Aldo Tonon.

The authors confirm that they, and/or their company or organization, hold copyright on all of the original material included in this paper. The authors also confirm that they have obtained permission, from the copyright holder of any third party material included in this paper, to publish it as part of their paper. The authors confirm that they give permission, or have obtained permission from the copyright holder of this paper, for the publication and distribution of this paper as part of the ICAS2012 proceedings or as individual off-prints from the proceedings.

References

- [1] Bowers A, Pahle J. *Thrust vectoring on the NASA F-18 high alpha research vehicle*, Volume 4771 di NASA technical memorandum, 1996.
- [2] Berrier B, Mason M. "Static performance of an axisymmetric nozzle with post-exit vanes for multi-axis thrust vectoring", NASA Technical Paper 2800, 1988.
- [3] Chiesa S, Corpino S, and Medici G. "System Programmable Logic Computer Aided Development Procedure", 8th ACD2010 European Workshop on Advanced Control and Diagnosis, Ferrara, 2010, pp. 229-234.
- [4] Chiesa S, Farfaglia S, and Viola N. "Design of all electric secondary power system for future advanced MALE UAV", 27th International Congress of the Aeronautical Sciences, Nice, 2010, pp. 1-10.
- [5] Davidson C, and McWhinnie J. "Engineering the control software development process", Factory 2000 - The Technology Exploitation Process, Fifth International Conference, 1997, Cambridge, Vol. 1, Pag 247-250.
- [6] Farfaglia S, Tranchero B, and Chiesa S. "The SAVE project: hypothesis and investigation strategies for alternative energy based systems for MALE UAV", 20th National Congress AIDAA, Milan, 2009, pp. 1-18.
- [7] Fielding D, Topps J. "Thermodynamic Data for the Calculation of Gas Turbine Performance", Aeronautical Research Council Reports and Memoranda, 1954.
- [8] Gilberl J, and Diehl G. "Application of Programmable Logic Controllers to Substation Control and Protection", IEEE Transactions on Power Delivery, 1994, Vol. 9, pp. 384-388.
- [9] Keller J. "Interactive control system design", Control Engineering Practice, 2006, Vol. 14, pp. 177-184.
- [10] Kurzke J, Riegler C. "A New Compressor Map Scaling Procedure For Preliminary Conceptual Design of Gas Turbines", ASME TurboExpo, 2000, Munich, 2000-GT-0006.
- [11] Medici G, Viola N, Corpino S, Fioriti M. "Development and validation of on-board systems control laws", Aircraft Engineering and Aerospace Technology, Vol. 84, Issue 3, 2012, pp. 151-161.
- [12] Saravanamuttoo H. *Gas Turbine Theory*, 4th ed., Pearson Prentice Hall, Harlow, 2009.
- [13] Sieros G, Stamatis A, and Mathioudakis K. "Jet engine component maps for performance modeling and diagnosis", Journal of Propulsion and Power, Vol. 13, 1997, pp. 665-674.
- [14] Sog-Kyun Kim, Pilidis P, and Junfei Yin. "Gas Turbine Dynamic Simulation Using Simulink®", Society of Automotive Engineers, San Diego, 2000, ISSN 0148-7191.